Available online at www.sciencedirect.com
ScienceDirect
Developmental Biology 297 (2006) 158–171
DEVELOPMENTAL BIOLOGY
www.elsevier.com/locate/ydbio

Functions of the ecdysone receptor isoform-A in the hemimetabolous insect *Blattella germanica* revealed by systemic RNAi in vivo

Josefa Cruz, Daniel Mané-Padrós, Xavier Bellés *, David Martín *

Departament de Fisiologia i Biodiversitat Molecular, Institut de Biologia Molecular de Barcelona (CID, CSIC), Jordi Girona 18, 08034 Barcelona, Spain

Received for publication 21 November 2005; revised 22 June 2006; accepted 28 June 2006
Available online 7 July 2006

Abstract

The molecular basis of ecdysteroid function during development has been analyzed in detail in holometabolous insects, especially in *Drosophila melanogaster*, but rarely in hemimetabolous. Using the hemimetabolous species *Blattella germanica* (German cockroach) as model, we show that the ecdysone receptor isoform-A (BgEcR-A) mRNA is present throughout the penultimate and last nymphal instars in all tissues analyzed (prothoracic gland, epidermis and fat body). To study the functions of *BgEcR-A*, we reduced its expression using systemic RNAi in vivo, and we obtained knockdown specimens. Examination of these specimens indicated that BgEcR-A during the last nymphal instar is required for nymphal survival, and that reduced expression is associated with molting defects, lower circulating ecdysteroid levels and defects in cell proliferation in the follicular epithelium. Some BgEcR-A knockdown nymphs survive to the adult stage. The features of these specimens indicate that BgEcR-A is required for adult-specific developmental processes, such as wing development, prothoracic gland degeneration and normal choriogenesis.

Keywords: Ecdysone receptor; Nuclear hormone receptor; *Blattella germanica*; 20-hydroxyecdysone; RNAi

Introduction

In insects, major developmental transitions occur throughout life cycles and are regulated by changes in the titer of the ecdysteroid hormone 20-hydroxyecdysone (20E) and its corresponding receptor. According to the first studies carried out on *Drosophila melanogaster*, 20E binds to its receptor, a heterodimeric combination of two transcription factors: the ecdysone receptor (EcR) and the retinoid X receptor (RXR)-homologue ultraspiracle (USP) (Yao et al., 1993). The activated heterodimeric receptor induces the expression of a number of primary response genes encoding transcription factors, like *E75*, *E74* and *Broad*, which in turn regulate secondary response genes and the metamorphosis process (reviewed by Thummel, 1995; Riddiford et al., 2001; King-Jones and Thummel, 2005). In *D. melanogaster*, part of the developmental specificity elicited by 20E is achieved by three EcR isoforms, EcR-A, EcR-B1 and EcR-B2 (Koelle et al., 1991; Talbot et al., 1993), that are expressed in a tissue-specific and developmental stage-specific manner (Talbot et al., 1993). Mutations inactivating all three isoforms are embryonic lethal (Bender et al., 1997). When analyzed separately, the lethal period resulted to be different for each isoform mutation. *EcR-A* mutants arrested predominantly at early to mid-pupal stage, suggesting that this protein is necessary after the formation of the pupal body plan and before the differentiation of adult structures (Davis et al., 2005). *EcR-B1* and *EcR-B2* double mutants arrested during early larval development, and a small proportion of specimens that were able to progress failed to pupate (Schubiger et al., 1998), whereas *EcR-B1* single mutants did not pupate (Bender et al., 1997). These results have been confirmed by reducing *EcR* expression through double-stranded RNA (dsRNA) interference experiments in vivo, where insects expressing a heat-inducible

* Corresponding authors. Xavier Bellés is to be contacted at fax: +34 932045904. David Martin, fax: +34 932045904.
E-mail addresses: xbragr@cid.csic.es (X. Bellés), dmcagr@cid.csic.es (D. Martín).

0012-1606/$ - see front matter © 2006 Elsevier Inc. All rights reserved.
doi:10.1016/j.ydbio.2006.06.048

dsRNA for EcR showed severe defects in larval molting and metamorphosis. Some specimens failed to pupate, and those that entered the prepupae stage died, showing defects in larval tissue cell death and in adult morphogenesis (Lam and Thummel, 2000).

Molecular data on EcR function in primitive hemimetabolous insects is scarce, mainly due to the fact that these insects are not amenable to genetic analysis. Recently, the RNA interference (RNAi) technique has been applied not only to model organisms, such as *D. melanogaster* and the nematode *Caenorhabditis elegans* (Montgomery et al., 1998; Kennerdell and Carthrew, 2000), but also to non-model species, such as the cockroach *Periplaneta americana* (Marie et al., 2000), the mosquitoes *Anopheles gambiae* (Blandin et al., 2002) and *Aedes aegypti* (Shin et al., 2003) and the beetle *Tribolium castaneum* (Bucher et al., 2002; Tomoyasu and Denell, 2004).

In this paper, we report the first molecular dissection of EcR functions in hemimetabolous insects using RNAi. First, we cloned the homologue of the *D. melanogaster* EcR-A isoform from the German cockroach, *Blattella germanica*, (BgEcR-A), and we characterized its developmental expression profile, as well as the effect of 20E upon its expression. Then, we followed an RNAi in vivo approach that allowed us to efficiently and specifically disrupt *BgEcR-A* gene expression and to study its role in coordinating developmental processes in our cockroach model.

Materials and methods

Insects

Specimens of *B. germanica* were obtained from a colony reared in the dark at 30±1°C and 60–70% r.h. All dissections and tissue sampling were carried out on carbon dioxide-anesthetized specimens.

Cloning of BgEcR-A cDNA

The *B. germanica* EcR-A homologue was obtained by PCR using a cDNA template from 20E-treated UM-BGE-1 cells, following the methodology described by Maestro et al. (2005). Degenerate primers for BgEcR-A amplification were designed on the basis of conserved DNA-binding domain (DBD) sequence of insect homologues, as follows: forward (EcR-dF1), 5′-TGYGARGGNTGYAARGG-3′; reverse (EcR-dR1), 5′-CKRCAYTCYTGR-CAYTT-3′. The amplified fragment (114 bp) was subcloned into the pSTBlue-1 vector (Novagen) and sequenced. This was followed by 5′ and 3′ RACE (5′- and 3′-RACE System Version 2.0; Invitrogen) to complete the sequence. For 5′-RACE, the reverse primer was EcRR1, 5′-TACACTGCATTCTTTG-TAATGCTTCT-3′ and the nested primer was EcRR2, 5′-GACGGTG-AAGACAACCAGTCATC-3. For 3′-RACE, the forward primer was EcRF1, 5′-AGAAGCATTACAAAGAATGCAGTGTA-3′ and the nested primer was EcRF2, 5′-CACATTACGGAAATAACCATCCTTAC-3′. All PCR products were subcloned into the pSTBlue-1 vector (Novagen) and sequenced.

Translation in vitro

The entire BgEcR-A open reading frame (ORF) was amplified by PCR using the primers: forward (EcRF3), 5′-TACTCCGGAGGTAGCGTCATCAT-3′; and reverse (EcRR3), 5′-CACATGTGCCACCGCGTCATCA-3′, which spans the stop codon. Accutaq polymerase (Sigma) was used. A fragment of the expected size (1.9 kb) was subcloned into pSTBlue-1 (Novagen) and sequenced. The BgEcR-A cDNA was transcribed and translated using the TNT coupled reticulocyte lysate system (Promega), according to the manufacturer's instructions.

RT-PCR/Southern blot analyses

Given the extremely low expression levels of transcription factors, a semi-quantitative RT-PCR/Southern blot approach was used (Maestro et al., 2005). Total RNA was extracted from different tissues using the GenElute™ Mammalian Total RNA kit (Sigma). Each of the RNA preparation (0.3–1 μg) was used for cDNA synthesis, as previously described (Maestro et al., 2005). For BgEcR-A mRNA detection, cDNA samples were subjected to PCR amplification with a number of cycles within the linear range of amplification (number of cycles ranging from 18 to 28, depending on the tissue and physiological stage) at 94°C for 30 s, 64°C for 30 s and 72°C for 45 s. The following primers were designed to amplify a sequence within the specific A/B domain: forward (EcRF1), 5′-TACTCCGGAGGTAGCGTCAT-CAT-3′; and reverse (EcRR4), 5′-GACGGTGAAGACAACCAGTCATC-3′. To amplify all possible BgEcR isoforms, a primer pair that amplified a fragment within the common ligand-binding domain (LBD) was used (BgEcRcom): forward (EcRFc1), 5′-GACAAACTCCTCAGAGAAGAT-CAAA-3′; and reverse (EcRRc2), 5′-TGATGACGCGGTGGCACATGTG-3′. To amplify BgRXR-S (Maestro et al., 2005), a primer pair that amplified a fragment within the LBD was used: forward (RXRF3), 5′-ATAATTGA-CAAGAGGCAGAGGAA-3′; and reverse, (RXRR4), 5′-TGGTCACTAA-GAGGCAAGGTAGT-3′. To amplify BgE75A and BgE75B, primer pairs that amplified their respective A/B-specific domain were used: forward for BgE75A (E75AF1), 5′-TTAGTGCTAGTGCAATGTGCTATTGA-3′; forward for BgE75B (E75BF1), 5′-CTAACGCTCCGCAATCCAGTTCA-3′; and the common reverse, (E75R1), 5′-ATGGAGCACTGTTGGTTCTTGGTA-3′. The PCR conditions were the same as those described above. As a reference, the actin 5C transcript of *B. germanica* was amplified by PCR using the same cDNA template samples (Maestro et al., 2005). Southern blot probes were generated by PCR with the same primer pairs using plasmid DNAs containing the corresponding cDNA clones as a template. The probes were labeled with fluorescein using the Gene Images random prime-labeling module (Amersham Biosciences). RT-PCR followed by Southern blotting of total RNA without reverse transcription did not result in amplification, indicating that there was no genomic contamination.

Whole-mount hybridization in situ

Digoxigenin-labeled RNA probes (sense and antisense) were generated by transcription in vitro using SP6 or T7 RNA polymerases (Roche). For the BgEcR-A probe, a 527-bp fragment containing the specific A/B domain was used. For hybridization in situ, tissues were dissected in Ringer's saline and fixed for 1 h with 4% paraformaldehyde in PBS. Tissues were washed in PBT (PBS; 0.2% Tween-20), treated with 40 μg/ml Proteinase K for 10 min, washed for 5 min in 2 mg/ml glycine in PBT, washed for 5 min in PBT and refixed for 20 min. After additional washes with PBT, the tissues were prehybridized in HS solution (50% formamide; 5× SSC; 50 μg/ml heparin; 0.1% Tween 20; 100 μg/ml sonicated and denatured ssDNA; 100 μg/ml tRNA from yeast (SIGMA)) at 56°C for 2 h. After prehybridization, BgEcR-A sense or antisense probes were added to the HS solution and incubated overnight at 56°C. Tissues were then successively washed in HS for 20 min, HS:PBTB/N (1:1) (0.2% Tween 20; 1% BSA; 10% inactivated normal goat serum in PBS) for 20 min and PBTB/N for 5 min. Samples were then blocked in PBTB/N for 2 h at room temperature. Tissues were incubated with the alkaline phosphatase-conjugated anti-digoxigenin antibody (preabsorbed with tissues of interest before hybridization) diluted 1:1000 in PBTB/N overnight at 4°C. Finally, tissues were washed in PBT for 2 h and hybridization was detected with the DIG Nucleic Acid Detection Kit (Roche), according to the manufacturer's instructions. Samples were mounted in 90% glycerol in PBS and examined using a Zeiss Axiophot microscope.

Incubation of fat body in vitro

Dorsal segments of the abdominal region, with their epidermis and adhering fat body tissue, were dissected from 1-day-old sixth instar female nymphs and

incubated in 1 ml of Grace's medium, with L-glutamine and without insect hemolymph (Sigma) at 30°C in the dark. For hormonal treatments, 20E (Sigma) was dissolved in water with 10% ethanol. 10^{-4}M cycloheximide (Chx) (Sigma) was used to reversibly inhibit protein synthesis (Comas et al., 2001). The incubation medium was changed every 5 h. At indicated time intervals, total RNA was isolated from the incubated fat body and BgEcR-A mRNA levels were estimated by RT-PCR amplification followed by Southern blotting.

Synthesis of double-stranded (ds) RNA and injection

To prepare the dsRNA targeted to BgEcR-A (dsBgEcR-A), a 700-bp *Eco*RI–*Bam*HI fragment encompassing the A/B domain of BgEcR-A was subcloned into the pSTBlue-1 vector (Novagen). Similarly, a 570-bp DNA sequence within the LBD region (from amino acid 381 to 570) was selected to prepare a dsRNA that would knockdown all possible BgEcR isoforms (dsBgEcRcom). Control dsRNA consisted of a non-coding sequence from the pSTBlue-1 vector (dsControl). Single-stranded sense and antisense RNAs were obtained by transcription in vitro using either SP6 or T7 RNA polymerases from the respective plasmids, and resuspended in water. To obtain the dsRNAs, equimolar amounts of sense and antisense RNAs were mixed, heated at 90°C for 5 min, cooled slowly to room temperature and stored at −20°C until use. Formation of dsRNA was confirmed by running 1 μl of the reaction products in 1% agarose gel. dsRNAs were suspended in diethyl pyrocarbonate-treated water and diluted in Ringer saline to a final concentration of 1 μg/μl, and 1 μl of the solution was injected in the abdomen of females that had just molted into sixth instar nymphs or into adults.

Microscopy and histological studies

All dissections were carried out in Ringer's saline. Mouthparts, digestive tract and trachea were directly immersed in 50% glycerol and examined microscopically. To study cuticle layers, a portion of abdominal ventral cuticle was fixed in 4% paraformaldehyde, dehydrated and embedded in paraffin. Cuticle sections (6 μm) were stained with toluidine blue. Ovaries were fixed in 4% paraformaldehyde, rinsed with PBS–0.2% Tween (PBT) and incubated for 20 min in 300 ng/ml phalloidin-tritc (Sigma) in PBS, and for 10 min in 1 μg/ml DAPI in PBT. After two washes with PBT, the tissues were mounted in Mowiol (Calbiochem). Prothoracic glands were dissected in PBS and directly incubated in LysoTracker Red DND-99, which labels acidic organelles, such as lysosomes (Rusten et al., 2004; Scott et al., 2004) in PBS (Molecular Probes, 1:1000 dilution) for 2 min and in 1 μg/ml DAPI in PBT for 10 min, and they were then washed with PBT and mounted in Mowiol. BrdU staining of nymphal ovaries was used for identification of cells in the S phase. Six-day-old sixth instar nymphs were injected with BrdU (Amersham) and maintained for 2 h. Ovaries were then dissected and fixed for 30 min in Carnoy (3 ethanol:1 acetic acid:1 water), washed three times in PBS and hydrolyzed with 2 N HCl for 30 min. They were then incubated with primary antibody diluted 1:1000 in PBSTB (PBS, 0.5% Triton, 0.2%BSA) at 27°C for 4 h, washed with PBS, subsequently incubated with peroxidase anti-mouse IgG (Sigma) (1:50 in PBSTB) for 4 h at 27°C and finally revealed with DAB (Amersham) for 5 min. All samples were examined with a Zeiss Axiophot microscope.

Quantification of ecdysteroids and protein contents, and characterization of vitellin

Hemolymph ecdysteroids were quantified by ELISA following the procedure described by Porcheron et al. (1989), and adapted to *B. germanica* by Pascual et al. (1992) and Romañá et al. (1995). 20E (Sigma) and 20E-acetylcholinesterase (Cayman) were used as standard and enzymatic tracer, respectively. The antiserum (AS 4919, kindly supplied by Prof. P. Porcheron, Université de Paris 6) was used at a dilution of 1:50,000. Absorbances were read at 450 nm using a Multiscan Plus II Spectrophotometer (Labsystems). The ecdysteroid antiserum has the same affinity for ecdysone and 20E (Porcheron et al., 1989), but because the standard curve was obtained with the latter compound, results are expressed as 20E equivalents. Total soluble proteins from the ovary were quantified according to Bradford (1976). SDS–PAGE of vitellin was carried out according to Martín et al. (1995).

Results

The nuclear hormone receptor cloned in B. germanica is an EcR-A homologue

Using an RT/PCR approach followed by 5′ and 3′ RACE, we isolated a 2.5-kb sequence encoding a polypeptide with a predicted molecular mass of 62.4 kDa. The putative start codon was preceded by an in-frame stop codon and the final stop codon was followed by a poly(A) sequence, indicating that it was a full-length ORF (GenBank Accession Number: AM039690). Amino acid sequence comparisons indicated that the protein had the domain organization characteristic of a nuclear hormone receptor. That is, a highly conserved ligand-independent A/B activation domain (amino acids 1–207); a two-zinc-fingered DBD (C domain, 208–276); a hinge region (D domain, 277–347); and a ligand-binding domain (LBD) (E domain, 348–568), which contained the putative ligand-dependent activation motif (Fig. 1A). Sequence comparison indicated that it was an EcR homologue, and the alignment of the A/B domain of our sequence with other EcR sequences indicated that the cloned cockroach cDNA encodes an EcR-A isoform (Fig. 1B). To determine whether the cloned cDNA contained a translatable ORF, it was expressed in a coupled TNT system under the control of the SP6 promoter. SDS–PAGE and fluorography showed that the molecular size of the protein synthesized in vitro closely corresponded to that expected, i.e., 66 kDa (Fig. 1C).

mRNA levels of BgEcR-A during the two last nymphal instars

In order to obtain expression profiles of *BgEcR-A*, mRNA levels were studied by semiquantitative RT/PCR followed by Southern blot using a primer pair targeted to the A/B domain of the sequence (Fig. 2A). Expression patterns were obtained in the prothoracic gland, the only tissue responsible for the synthesis of ecdysteroids during nymphal development, and the epidermis, the tissue responsible of cuticle synthesis, as well as in the fat body and ovaries, during the fifth and sixth nymphal instars of *B. germanica*. BgEcR-A mRNA was present in similar amounts in both developmental stages and in all tissues (Fig. 2B, lower panel). In addition, we performed RT-PCR/Southern blot with a primer pair designed to amplify a sequence within the LBD and hence, able to detect all possible BgEcR isoforms (BgEcRcom; Fig. 2A). The expression pattern of BgEcRcom was the same than that described for BgEcR-A in prothoracic gland and epidermis (Fig. 2B) and in the fat body and ovaries (data not shown). These patterns contrast with that of hemolymph ecdysteroid titer, which shows a characteristic cycle in nymphal stages, peaking three days before each molt (Fig. 2B, upper panel; data from Cruz et al., 2003). To further characterize the spatial distribution of the BgEcR-A transcript, hybridization in situ of nymphal tissues was performed. Strong *BgEcR-A* expression was observed in all cells of the prothoracic gland (Fig. 2C), the

Fig. 1. (A) Amino acid sequence of the *B. germanica* ecdysone receptor isoform-A (BgEcR-A). The DNA-binding domain is underlined and the ligand-binding domain is dotted underlined. (B) Comparison of the A/B domain of BgEcR-A with that from other insect species. *Locusta migratoria* (LmEcR-A), *D. melanogaster* (DmEcR-A), *Ceratitis capitata* (CcEcR-A), *Manduca sexta* (MsEcR-A), *Bombyx. mori* (BmEcR-A) and *A. aegypti* (AaEcR-A). The conserved 20 amino acid sequence at the C-terminal of the A/B domain of all isoform-A receptors (specific A-box) is indicated. (C) Translational analysis in vitro. The cDNA clone encoding BgEcR-A was translated by a coupled transcription-translation system in vitro and labeled by [^{35}S]-methionine. The translation product was resolved by SDS–PAGE using a 10% gel followed by autoradiography. Molecular mass standards are shown on the right.

fat body (Fig. 2D) and the follicular cells surrounding the basal oocyte (Fig. 2E, arrowhead) from 6-day-old sixth instar nymphs. Sense probe resulted in no detectable staining in the fat body (Fig. 2F), as well as in the prothoracic gland and the follicular cells (data not shown).

20E does not affect BgEcR-A expression

The expression pattern of the *BgEcR-A* gene in the tissues studied suggests that it is not regulated by 20E. To test this hypothesis, we studied the BgEcR-A mRNA levels in dorsal abdominal segments with their epidermis and with adhering fat body tissue from sixth instar female nymphs incubated in vitro for 1–24 h in the presence of either 20E (5×10^{-6}M), the protein synthesis inhibitor Chx (10^{-4}M) or both 20E and Chx. In all cases, BgEcR-A transcript levels remained unchanged (Fig. 2G). The same result was obtained when the epidermis with adhering fat body was incubated for 10 h with increasing concentrations of 20E, from 10^{-8} to 10^{-5}M. Again, the same results were obtained when we used the primer pair combination (BgEcRcom) designed to detect all possible BgEcR isoforms (data not shown).

RNAi in nymphs reduces BgEcR-A mRNA levels and impairs the expression of 20E-dependent genes

To study the function of BgEcR-A during nymphal development, *BgEcR-A* expression was lowered by RNAi. The 700-bp interfering dsRNA (dsBgEcR-A; Fig. 3A) was injected into the abdomen of freshly ecdysed last instar female nymphs, and mRNA levels were determined in the prothoracic gland and in the epidermis with adhering fat body 8 days later. Specimens injected with dsControl were used as negative controls. Results showed that BgEcR-A mRNA levels decreased substantially in the dsBgEcR-A-treated insects compared to controls (Fig. 3B).

To verify that BgEcR-A is essential to transduce the ecdysteroidal signal in *B. germanica*, we studied the expression of two genes involved in that transduction in dsBgEcR-A-treated sixth instar nymphs, i.e., *BgRXR-S* (which encodes the heterodimeric partner of BgEcR) and *BgE75* (a 20E-regulated gene). In our laboratory, we have cloned two isoforms of the nuclear receptor E75, namely BgE75A (accession number: AM238653) and BgE75B (accession number: AM238654), and we have shown that the expression of both is dependent of 20E (D. M-P., X.B. and D. M., unpublished results). Prothoracic gland RNA was obtained from 6-day-old sixth instar nymphs that had been treated with dsControl or dsBgEcR-A at the beginning of the instar. The expression of *BgRXR-S*, *BgE75A* and *BgE75B* was then analyzed by RT-PCR/Southern blot (Fig. 3C). As expected, BgEcR-A mRNA levels clearly decreased in the dsBgEcR-A-treated nymphs whereas those of BgRXR-S were unaffected. Most importantly, the expression of *BgE75A* and *BgE75B* were dramatically reduced in the dsBgEcR-A-treated nymphs. The same result was obtained when the expression of these factors was analyzed in the fat body and the epidermis (data not shown).

BgEcR-A knockdowns exhibit defects in molting

Sixth (last) instar nymphs that had been treated with dsBgEcR-A when freshly ecdysed had normal appearance and

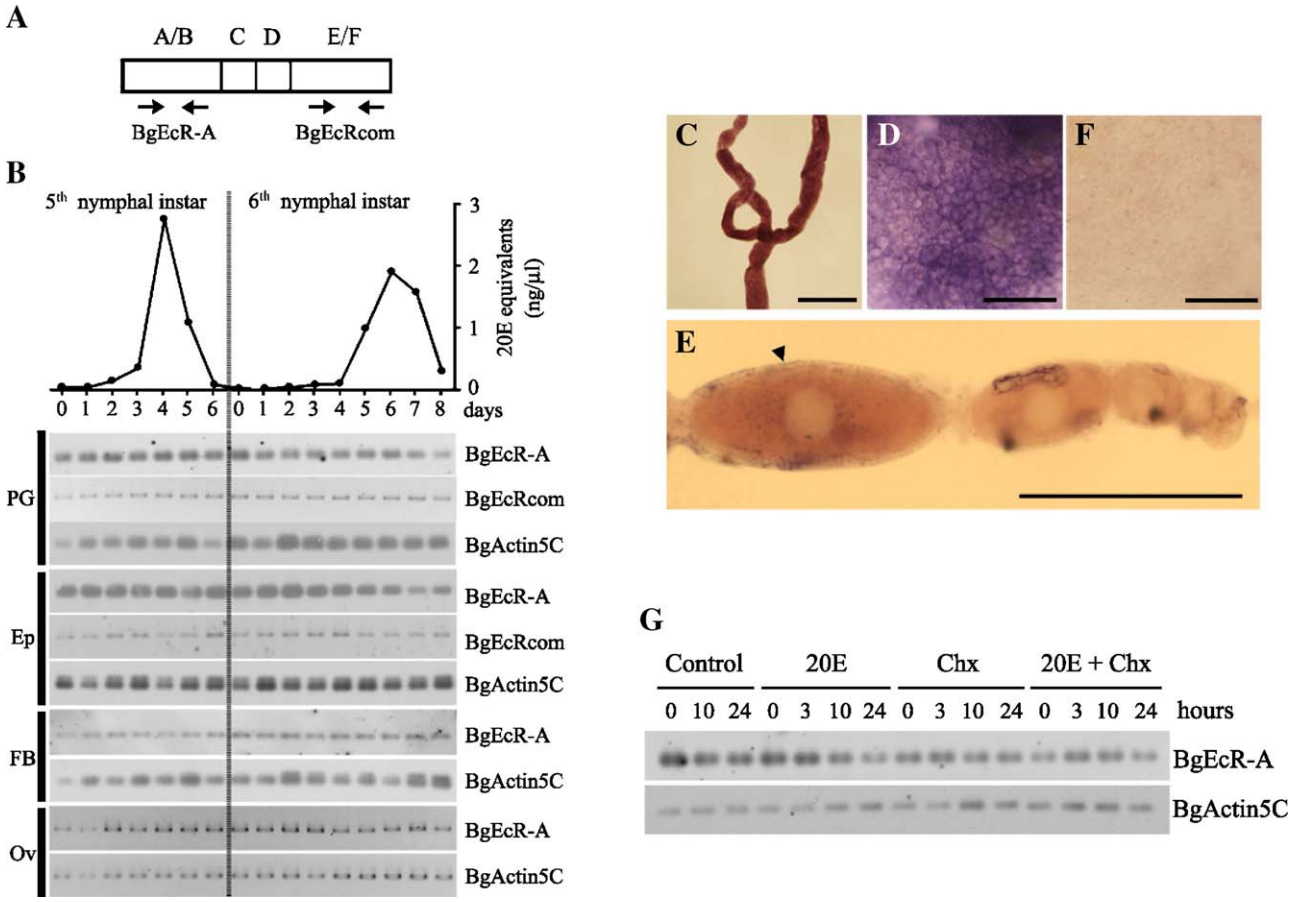

Fig. 2. Expression patterns of BgEcR-A and BgEcRcom mRNAs in different tissues of *B. germanica* and effect of 20-hydroxyecdysone (20E) and cycloheximide (Chx) on BgEcR-A mRNA levels. (A) Schematic representation of BgEcR-A showing the position of the primer pairs used in the analysis. (B) BgEcR-A and BgEcRcom mRNA levels studied in prothoracic gland (PG), epidermis (Ep), fat bodies (FB) and ovaries (Ov) (lower panel) and hemolymph ecdysteroid contents during these stages (upper panel). Data of hemolymph ecdysteroid levels are from Cruz et al. (2003). The Southern blots are representative of three replicates. (C–E) Hybridization in situ of different tissues from a 6-day-old sixth instar nymph using an antisense BgEcR-A RNA probe. (C) mRNA of BgEcR-A is present in the prothoracic gland, (D) in the fat body and (E) in the follicular epithelium surrounding the basal oocytes (arrowhead). (F) Control fat body hybridized with a sense BgEcR-A probe showing no staining. Scale bars: 250 µm in panels C, D and F; 500 µm in panel E. (G) Fat bodies with the adhered epidermis from sixth instar female nymphs were incubated and treated with either 5×10^{-6}M 20E; 10^{-4}M cycloheximide (Chx); or both 20E and Chx for the time periods shown. Equal amounts of total RNA from staged nymphs and from fat bodies incubated in vitro were analyzed by RT-PCR/Southern blotting using BgEcR-A and BgEcRcom-specific probes. BgActin5C levels were used as a reference. The Southern blots are representative of three replicates.

behavior until the end of the instar. At day 8 after treatment, 58% of them ($n=180$) did not molt into adults, and 24–48 h later they were motionless, failed to respond to any stimulus and became arrested (Figs. 4A and B). Conversely, 100% of the dsControl-treated nymphs ($n=144$) molted normally into adults. Most of the arrested specimens died within 24–48 h and, remarkably, they had the structures of ectodermal origin duplicated (of nymphal and adult nature). In the cephalic region, for example, two superimposed pairs of mandibles, antennae, as well as two laciniae were apparent (Figs. 4C–E). Moreover, they showed a double superimposed tracheal system, with the old trachea visible in the lumen of the new ones (Fig. 4F). The foregut and hindgut portions of the digestive tract were also duplicated (images not shown).

Histological sections showed both endocuticle and exocuticle layers present in the abdomen of dsControl and of dsBgEcR-A-treated specimens on the last day of the sixth nymphal instar (Figs. 4G and H). One day later, the dsControl specimens molted normally, but the dsBgEcR-A-treated specimens were unable to ecdyse and arrested. Forty-eight hours after arresting, the nymphal endocuticle of dsBgEcR-A knockdowns had been degraded, and only the exocuticle was observed (Fig. 4I).

In an equivalent series of experiments, we injected dsBgEcRcom, which would interfere not only the BgEcR-A isoform but also any other possible occurring BgEcR isoform. At day 8, 89% of the dsBgEcRcom-treated specimens ($n=45$) became arrested and exhibited duplicated ectodermal structures, exactly as in the dsEcR-A-treated specimens.

BgEcR-A knockdown nymphs produce less ecdysteroids

The fact that dsBgEcR-A-treated nymphs failed to molt and arrested before adult ecdysis suggested that these specimens had the ecdysteroid levels altered, in addition to have less BgEcR-A. To test this hypothesis, we determined

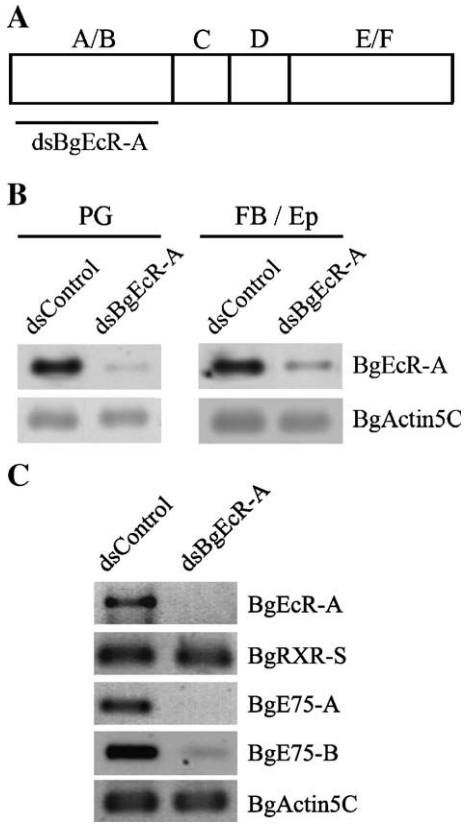

Fig. 3. RNAi of BgEcR-A in sixth instar female nymphs of *B. germanica*. (A) Schematic representation of BgEcR-A showing the region used to generate the dsRNA. (B) 1 μg of dsRNA from BgEcR-A (dsBgEcR-A) or from a non-specific sequence (dsControl) was injected in sixth instar female nymphs, and BgEcR-A mRNA levels were measured 8 days later from prothoracic gland (PG) and fat bodies with adhered epidermis (FB/Ep) by RT-PCR/Southern blotting using BgEcR-A-specific probes. BgActin5C levels were used as a reference. The Southern blots are representative of six replicates. (C) RNAi of BgEcR-A in sixth instar female nymphs inhibits BgE75A and BgE75B expression. 1 μg of dsRNA from BgEcR-A (dsBgEcR-A) or from a non-specific sequence (dsControl) was injected in sixth instar female nymphs, and levels of BgEcR-A, BgRXR-S, BgE75A and BgE75B mRNAs were measured 6 days later from prothoracic gland by RT-PCR/Southern blotting using specific probes. BgActin5C levels were used as a reference. The Southern blots are representative of six replicates.

the ecdysteroid titer in the hemolymph of sixth instar nymphs at days 5 and 6; that is, when ecdysteroids reach the highest levels during the nymphal instar (Cruz et al., 2003). As shown in Fig. 5, whereas in dsControl-treated nymphs ecdysteroid levels were high at day 6, as expected, those in dsBgEcR-A-treated nymphs remained significantly low, showing a 66% reduction with respect to controls.

BgEcR-A controls cell proliferation in the follicular epithelium

B. germanica ovary is panoistic and does not contain nurse cells. Each oocyte is surrounded by a monolayer of follicular cells, and only the basal oocyte of each ovariole experiences a significant growth during the last nymphal instar (Fig. 6A, arrowhead), whereas the remaining ones remain immature (Fig. 6A, bracket). Basal oocyte growth during the last nymphal instar is due to cell proliferation in the follicular epithelium, from ca. 500 to ca. 4000 cells (J.C, D.M. and X.B., unpublished results). In order to analyze whether BgEcR-A controls such an increase, we used the incorporation of BrdU as a marker of cell proliferation in oocytes of dsControl and dsBgEcR-A nymphs at day 6. We found significant BrdU-labeled nuclei scattered throughout basal oocytes of dsControl nymphs at day 6. Labeled cells were also observed in sub-basal oocytes, although label was lighter (Fig. 6A). Conversely, ovaries from dsBgEcR-A-treated nymphs of the same age did not show BrdU-labeled cells (Fig. 6B), thus indicating that BgEcR-A is required for follicular cell proliferation during nymphal development. As a result of cell proliferation impairment in the follicle, ovaries from dsBgEcR-A-treated nymphs contained a significant lower number of follicular cells when compared with control specimens (cell mean number in dsControl: 3281 ± 190; in dsBgEcR-A: 2510 ± 156; $n = 7$ and 5, respectively, t test, $p \leq 0.006$). In addition, oocytes were smaller (mean length in dsControl: 396.15 ± 7.14 μm; in dsBgEcR-A: 349.94 ± 11.66 μm; $n = 7$ and 5, respectively, t test, $p \leq 0.007$).

BgEcR-A is involved in wing extension and prothoracic gland degeneration

A total of 42% of the dsBgEcR-A-treated nymphs molted to adult, thus allowing the study of BgEcR-A functions in this stage. In hemimetabolous insects, the adult molt is characterized by a limited set of morphological and physiological changes. In addition to wing extension and degeneration of the prothoracic gland, the adult female is also characterized by the synthesis of yolk proteins in the fat body and its incorporation into developing oocytes.

All dsBgEcR-A-treated nymphs that molted into adults showed deformations in the fore- and hindwings (Figs. 7A and B), ranging from moderate defects (Fig. 7, compare C, F to D, G) to a completely unextended wing phenotype (Figs. 7E and H). In addition, and concerning the external morphology, a small number of dsBgEcR-A-treated specimens showed the hind tarsi correctly patterned, but shorter with respect to controls (Fig. 7B).

In dsControl specimens, the prothoracic gland had lost turgidity 48 h after the adult molt, cell density decreased, and by day 7 the gland became reduced to a central muscular axis surrounded by a very low number of cells (Figs. 8A and B; see also Romañá et al., 1995). Conversely, the prothoracic gland failed to degenerate and was observed in apparent good shape (Figs. 8C and D) in the dsBgEcR-A-treated specimens. In order to study the degeneration of the prothoracic gland, we used the specific fluorescent dye Lysotracker Red, which labels acidic organelles, such as lysosomes, and is currently used as a test for autophagy (Rusten et al., 2004; Scott et al., 2004). In 3-day-old dsControl adult females, the prothoracic gland showed clear lysotracker staining (Fig. 8E), thus indicating that the gland was rapidly degenerating by autophagy. Conversely, the prothoracic gland of dsBgEcR-A knockdowns did not incorporate lysotracker and displayed only a faint, diffuse staining (Fig. 8F). It is worth noting, however, that the

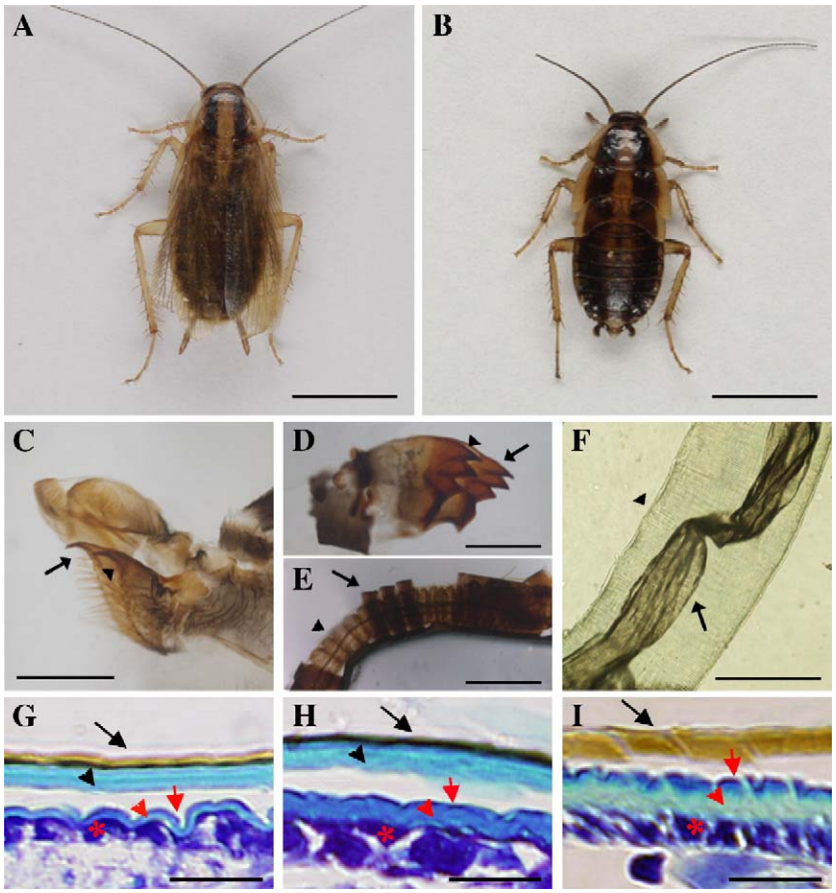

Fig. 4. Effect of RNAi-mediated knockdown of BgEcR-A in molting of *B. germanica*. Sixth instar female nymphs were injected with 1 μg of dsBgEcR-A or with dsControl at day 0 and left until the imaginal molt 8 days later. (A) dsControl specimen 1 day after the imaginal molt, showing a normal adult appearance. (B) dsBgEcR-A specimen at the same time point arrests the molting process. The arrested specimens show duplication of cuticular structures, like (C) double laciniae (see the nymphal, arrow, and adult, arrowhead, laciniae), (D) two mandibles, (E) two antenna and (F) two trachea of the same specimen. (G–I) histological sections of the cuticles of dsBgEcR-A nymph knockdowns. (G) dsControl sixth instar nymph cuticle on day 8. (H) dsBgEcR-A specimen on day 8, just before adult ecdysis. (I) dsBgEcR-A specimen 48 h after arresting. Epicuticle (arrows), endocuticle (arrowheads) and epidermis (asterisks) are indicated. Black arrows and arrowheads represent nymphal epi- and endocuticle. Red arrows and arrowheads represent adult epi- and endocuticle. Scale bars: 5 mm in panels A and B; 500 μm in panels C–E; 200 μm in panel F; 50 μm in panels G–I.

persistent prothoracic gland of dsBgEcR-A-treated specimens was inactive because hemolymph ecdysteroid titers of these specimens were as low as those of controls (data not shown).

BgEcR-A is required for choriogenesis during adult development

In *B. germanica*, oogenesis occurs during the adult stage. During this period, only the basal oocyte of each ovariole matures and growths (Fig. 9A, arrowhead) due to the incorporation of yolk proteins synthesized in the fat body in a juvenile hormone-dependent manner (Comas et al., 2001). The remaining oocytes of the ovariole keep immature (Fig. 9A, bracket). During vitellogenesis, the follicular cells surrounding the basal oocyte show huge and binucleate nuclei (Figs. 9B and D) and prominent F-actin filaments at their periphery (Figs. 9C and D). When maturation is completed, basal oocytes form the chorion and are oviposited into an ootheca, which is transported by the female attached to the genital atrium until egg hatching.

We observed that none of the dsBgEcR-A-treated nymphs that molted into adults produced the ootheca at the end of the first gonadotrophic cycle. Upon dissection of these specimens, DAPI and phalloidin-tritc staining revealed that follicular cells of the basal oocytes had degenerated (data not shown). As a first step to characterize this phenotype, we analyzed the expression pattern of the *BgEcR-A* gene in the adult ovary. RT-PCR/Southern blot analysis showed that the BgEcR-A was expressed throughout the adult stage, although mRNA levels decreased towards the end of the first gonadotrophic cycle (Fig. 9E). This concurs with our earlier finding that the EcR heterodimeric partner BgRXR-L is also present in the ovary (Maestro et al., 2005), suggesting that a fully functional receptor is required during all stages of oocyte development. To characterize the spatial distribution of *BgEcR-A* expression in the ovary of *B. germanica*, we carried out an analysis of hybridization in situ. BgEcR-A transcripts were detected in the cytoplasm of the follicular cells from 5-day-old adult females (Figs. 9F and G). The same spatial distribution was observed in ovaries from newly emerged and in 7-day-old adult females

(data not shown). Moreover, BgEcR-A mRNA was also clearly visible in the follicular cells of the sub-basal oocytes, and even in the more immature ones, but it was absent in the germarium and the terminal filament (Fig. 9H). Equivalent experiments using the sense probe resulted in no detectable staining (Fig. 9I).

To characterize the function of BgEcR-A in the ovary, freshly ecdysed adult females were treated with dsBgEcR-A, which clearly reduced the levels of BgEcR-A mRNA in the ovary on day 6, compared to controls (Fig. 10A). As a consequence, none of the dsBgEcR-A-treated females produced the ootheca ($n=26$). To study whether these effects were due to defects in the vitellogenic process, that is, in the synthesis of yolk protein precursors by the fat body and their incorporation into developing oocytes, we measured protein contents in ovaries from dsControl and dsBgEcR-A-treated females. Comparing ovaries from dsBgEcR-A and dsControl females, there were no significant differences neither in total protein contents (Fig. 10B), nor in vitellin (Fig. 10C), which is the major yolk protein in *B. germanica*. We then studied the structural changes in the follicular cells during oogenesis by staining the F-actin filaments with phalloidin-tritc (Figs. 10D–G). During early vitellogenesis, that is, between days 3 and 5, the follicular cells from dsControl specimens showed large intercellular spaces, facilitating the access of circulating vitellogenin to the oocyte (Fig. 10D). At this stage, follicular cells exhibited strong fluorescent labeling in their periphery due to the prominent double nuclei located in the center of the cell. Between days 6 and 7, at the onset of choriogenesis, the intercellular spaces disappeared and the follicular cells formed a continuous layer (Fig. 10E). On day 7, the F-actin filaments rearranged, forming parallel bundles across the apical surface of each follicular cell (Fig. 10F). At late choriogenesis, just before oviposition, the

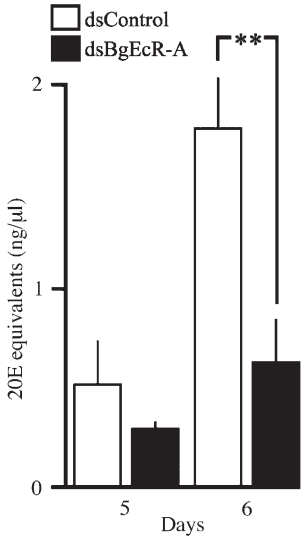

Fig. 5. Effect of RNAi-mediated knockdown of BgEcR-A on ecdysteroid levels in *B. germanica*. Hemolymph from dsBgEcR-A and dsControl-treated nymphs were collected at days 5 and 6, and ecdysteroid levels were determined by ELISA. Results are expressed as ng of 20-hydroxyecdysone (20E) equivalents. Vertical bars indicate the SEM ($n=8$–16). Asterisks indicate differences statistically significant at $p \leq 0.0039$ (t test).

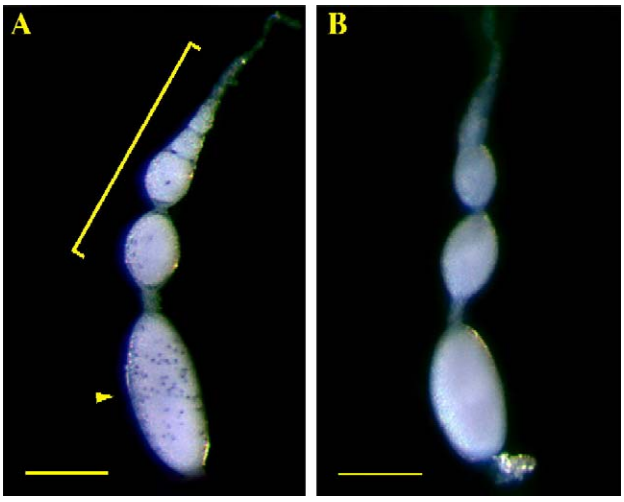

Fig. 6. Effect of RNAi-mediated knockdown of BgEcR-A on the proliferation of the follicular epithelium during nymphal development of *B. germanica*. dsControl and dsBgEcR-A-treated sixth instar nymphs were pulsed with BrdU on day 6 and ovaries were dissected and stained to reveal BrdU incorporation 2 h later. (A) Ovariole from dsControl 6-day-old nymph, showing abundant BrdU-labeled cells in the basal (arrowhead), sub-basal and even in more immature oocytes (bracket). (B) Ovariole from dsBgEcR-A nymph at day 6 showing no BrdU incorporation. Scale bars: 200 µm.

cells lost the hexagonal morphology, fuse each other and formed a squamous sheet (Fig. 10G). In ovaries from dsBgEcR-A-treated females, the same sequence of events was observed until the onset of choriogenesis, although with a delay of one day approximately (Figs. 10H–J). However, after the disappearance of the intercellular spaces at day 7, just at the onset of choriogenesis, follicular cells from dsBgEcR-A-treated specimens failed to rearrange the actin filaments, resulting in a disorganized actin structure (Fig. 10K). Finally, the cells did not fuse and the follicular epithelium degenerated (Fig. 11). Degeneration was evident given the irregular distribution of the nuclei of the follicular cells and their aberrant shape (Figs. 11A and B). Moreover, phalloidin-tritc staining of these ovaries also revealed that the follicle became disorganized (Figs. 11C and D). The degeneration was specific of the basal oocyte, the remaining oocytes of each ovariole being not affected.

Discussion

We present the first detailed report on the functions of EcR-A on nymphal and adult development in a hemimetabolous insect. The study is based on RNAi in vivo of EcR-A in the German cockroach, *B. germanica*. EcR-A of *B. germanica* (BgEcR-A) is very similar to the EcR-A of other insects, with a telltale tract of 20 amino acids at the carboxyl-end of its A/B-specific domain, which is highly conserved (Fig. 1). A distinguishing feature of BgEcR-A is that the carboxy-terminal end of the ligand-binding domain is very short (2 aa), contrasting with the longer F domain found in Lepidoptera and Diptera (from 18 aa in *M. sexta* to 226 aa in *D. melanogaster*).

The expression of *BgEcR-A* through the two last nymphal instars and in all tissues analyzed (prothoracic gland, epidermis, fat body and ovary), parallels that of its heterodimeric partner

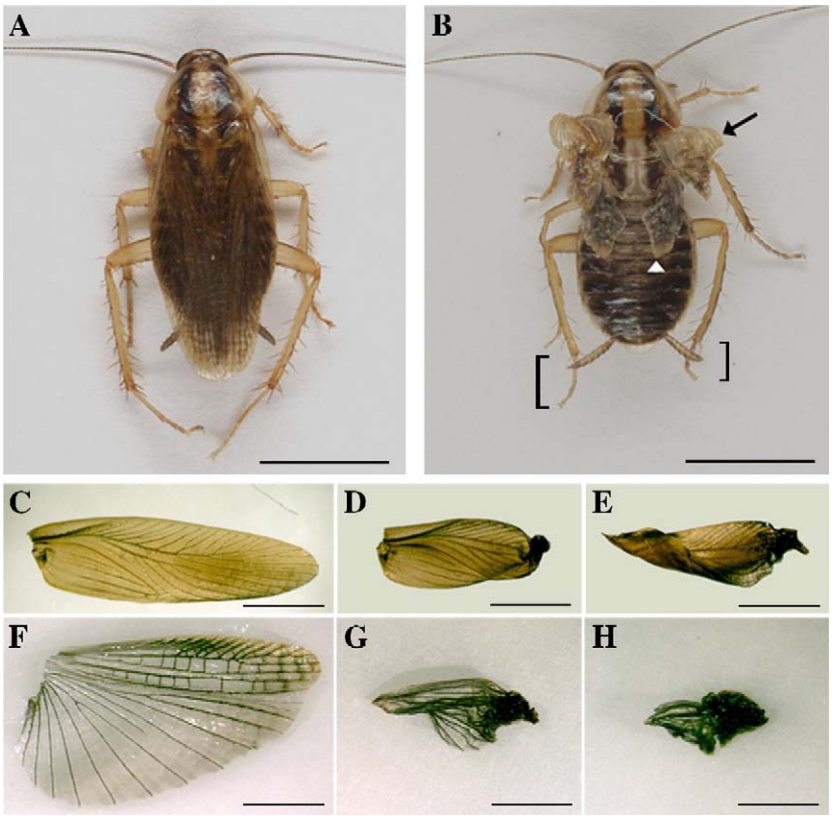

Fig. 7. Effect of RNAi-mediated knockdown of BgEcR-A in adult wing extension of *B. germanica*. (A) dsControl nymph 1 day after the imaginal molt, showing a normal adult appearance, with perfectly extended wings. (B) dsBgEcR-A nymph 1 day after the imaginal molt showing severe defects of wing extension in both the forewings (arrow) and hindwings (arrowhead). Some knockdown specimens display shorter tarsi (brackets). Wing extension phenotypes vary from moderately severe (compare normal, panels C and F, with interfered, panels D and G) to a totally unextended phenotype in both wing pairs (compare panels C and F with interfered panels E and H). Scale bars: 5 mm.

BgRXR (Maestro et al., 2005), suggesting that the fully functional 20E receptor is needed in nymphal development. The situation is quite different to the complex expression patterns of EcR isoforms observed in holometabolous insects during larval-pupal development. In *D. melanogaster*, *EcR-A* expression is very low during the second and third larval instars, but it is clearly induced at mid-prepupae, 10–12 h after the onset of puparium formation, in apparent response to a 20E pulse, whereas *EcR-B1* and *EcR-B2* isoforms are expressed at high levels at the end of the second and third larval instars (Sullivan and Thummel, 2003). In *M. sexta*, EcR-B1 predominates through the larval and pupal development, whereas expression of EcR-A is restricted to the onset of new cuticle synthesis during larval molts, and increases later than EcR-B1 during pupal and adult molts (Jindra et al., 1996). In contrast with holometabolous insects, the constitutive expression of *BgEcR-A* suggests that *B. germanica* does not rely on fine control of receptor transcription to regulate nymphal development. This conclusion is further supported by the lack of BgEcR-A mRNA induction upon incubation of fat body with adhered epidermis with 20E (Fig. 2G). Again, this is in contrast to many cases reported in holometabolous species, where 20E regulates *EcR* transcription. For example, *EcR* is rapidly induced by 20E in organs of third instar larvae of *D. melanogaster* incubated in vitro (Karim and Thummel, 1992). 20E-dependent *EcR* activation has been also described in the epidermis of *M. sexta* incubated in vitro (Jindra et al., 1996), in the silk gland of *Galleria mellonella* (Jindra and Riddiford, 1996), in the adult fat body of *A. aegypti* (Wang et al., 2002), in salivary glands of *C. capitata* (Verras et al., 2002) and in cultured cells of *Choristoneura fumiferana* (Kothapalli et al., 1995; Perera et al., 1999).

BgEcR-A is required during nymphal development

A consequence of reduced levels of BgEcR-A in last instar nymphs of *B. germanica* is the reduction of hemolymph ecdysteroid levels (Fig. 5). In general, the production of ecdysteroids by the prothoracic gland is triggered by the prothoracicotropic hormone (PTTH) produced in the brain and, in some cases such as *M. sexta*, stored in neurohemal organs like the corpora allata, from where it is released to the hemolymph (see Gilbert, 2004). The impairment of ecdysteroid synthesis in BgEcR-A knockdowns might be due to the fact that PTTH synthesis, release and/or function at the cellular level in the prothoracic gland are EcR-dependent processes. However, no *PTTH* gene has been identified in any insect species outside Diptera and Lepidoptera. Another level of ecdysteroid synthesis control is achieved by the action of several 20E-dependent factors in

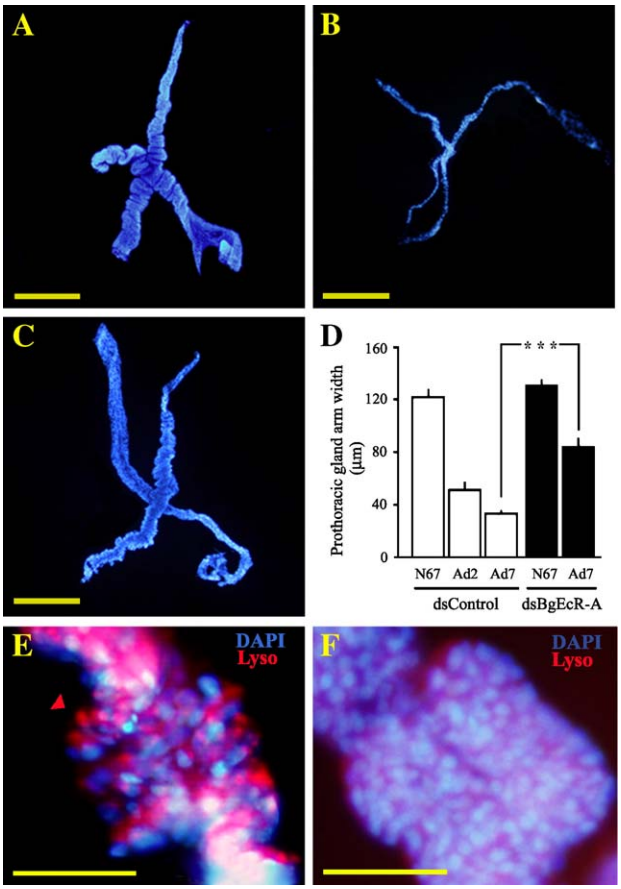

Fig. 8. Effect of RNAi-mediated knockdown of BgEcR-A on the degeneration of the prothoracic gland during the adult stage of *B. germanica*. Prothoracic glands from dsControl and dsBgEcR-A-treated nymphs were stained with DAPI to visualize the nuclei (A–C). (A) Prothoracic gland from dsControl sixth instar nymph, showing a normal appearance on day 7. (B) Prothoracic gland from dsControl sixth instar nymph 7 days after the imaginal molt, showing a dramatic reduction of its cellular mass. (C) Prothoracic gland from dsBgEcR-A sixth instar nymph that molted into adult, showing a normal prothoracic gland with no signs of degeneration 7 days after the imaginal molt. (D) Quantification of the degree of degeneration by measuring the arm widths of the prothoracic gland from dsControl and dsBgEcR-A-treated nymphs at different days. Vertical bars indicate the SEM ($n=9$–18). Asterisks indicate differences statistically significant at $p \leq 0.0001$ (t test). Prothoracic gland degeneration occurs by autophagy (E and F). (E) Prothoracic gland from dsControl-treated sixth instar nymph at day 3 after the imaginal molt, showing a strong lysotracker staining. (F) Prothoracic gland from dsBgEcR-A-treated sixth instar nymph at day 3 after the imaginal molt, showing a diffuse non-specific lysotracker staining. Scale bars: 200 µm in panels A–C, 50 µm in panels E and F.

the prothoracic gland. In *D. melanogaster*, for example, the orphan nuclear receptor E75A promotes the synthesis of ecdysteroids during larval development (Bialecki et al., 2002), whereas BR-Z3 acts as a negative regulator of this process (Zhou et al., 2004). In this sense, our results are compatible with these data because dsBgEcR-A-treated nymphs show much lower levels of BgE75A in the prothoracic gland at day 6 (Fig. 3C), just when control insects start ecdysteroid synthesis.

A second consequence of BgEcR-A reduction is that affected nymphs are unable to undergo normal molting, and arrest just before ecdysis. These specimens exhibit the typical "double mouthooks" phenotype characteristic of duplicated ectodermic structures, as in *D. melanogaster* mutants of genes involved in steroidogenesis, like *molting defective* (Neubueser et al., 2005) and *ecdysoneless* (Gaziova et al., 2004). These features show that treated nymphs are able to synthesize the new cuticle and to digest the old one correctly, but they cannot shed out the exuvia, a key step in the molting process. Shedding behavior is a sequential event of precise body contractions controlled by a number of peptides released from Inka cells (pre-ecdysis and ecdysis triggering hormones) and from the central nervous system (eclosion hormone), in response to sharp fluctuations in the levels of circulating ecdysteroids (for a review, see Zitnan and Adams, 2005). We propose that reduction of BgEcR-A, together with reduction of circulating ecdysteroids, leads to the incorrect synthesis and/or release of some of the molting peptides and, as a consequence, the nymph is unable to ecdyse properly and arrests.

In addition to exhibit molting problems, the BgEcR-A knockdown nymphs show a reduced number of follicular cells in the basal oocyte at the end of the sixth nymphal instar, suggesting that BgEcR-A is involved in follicle growth and maturation. The effect of BgEcR-A on cell proliferation has been shown to be complex in other insects. For example, proliferation is induced by ecdysteroids within the optic lobe anlagen during metamorphosis of *M. sexta* (Champlin and Truman, 1998), whereas proliferation of the IAL-PID2 cell line derived from imaginal wing discs of *Plodia interpunctella* is suppressed by the same hormones (Mottier et al., 2004).

BgEcR-A is required for adult development

The percentage of dsBgEcR-A-treated nymphs that completed the imaginal molt allowed us to identify BgEcR-A-dependent developmental processes in the adult. The most apparent defect observed in BgEcR-A knockdown adults was that all of them failed to extend both the fore- and hindwings correctly (Fig. 7). The severity of the phenotype varied somewhat, although the membranous hindwings were more often and more severely affected. In *D. melanogaster*, several reports have demonstrated that wing extension is controlled by neuropeptides. Two of these peptides, crustacean cardioactive peptide and bursicon, are released into the hemolymph after ecdysis, and directly control wing extension (Park et al., 2003; Dewey et al., 2004). Moreover, when neurosecretory cells expressing the eclosion hormone are ablated (McNabb et al., 1997), or a targeted EcR-dominant negative protein is over-expressed in these cells, thus blocking the 20E signaling cascade, pupa can molt into adult but fail to extend the wings (Cherbas et al., 2003). Based on the *D. melanogaster* model, we can consider wing extension a part of the ecdysis behavior program, and consequently it should be affected by the alteration of EcR-A levels in *B. germanica*.

The second effect observed in all BgEcR-A knockdown nymphs that molt into adults was that the prothoracic gland does not degenerate (Fig. 8). In the majority of insects, including *B. germanica* (Romañá et al., 1995), *D. melanogaster* (Dai and Gilbert, 1991) and *M. sexta* (Dai and Gilbert, 1997), the

prothoracic gland degenerates after metamorphosis or soon after the imaginal molt. In our control specimens, the prothoracic gland cells exhibit large amounts of lysosome-like structures, and the gland appears disintegrated 48 h after the imaginal molt, leaving only a thin muscular axis surrounded by a few cells (Fig. 8). This suggests that destruction of the gland proceeds by autophagy. In BgEcR-A knockdown insects, however, the formation of lysosomes is not observed, and the gland does not degenerate. This is the first report implicating EcR in the autophagic death of prothoracic gland, although EcR has been linked with developmental-stage-specific destruction of other tissues in *D. melanogaster*. For example, overexpression of isoforms of Broad, a 20E-dependent early gene, induces degeneration of the prothoracic gland portion of the ring gland (Zhou et al., 2004), and a pulse of 20E causes the autophagic destruction of the salivary glands, which degenerate very rapidly at the onset of pupal stage (reviewed in Thummel, 2001; Yin and Thummel, 2005). Other 20E-controlled factors like BR-Z1, βFTZ-F1, E74A and E93 have also been involved in controlling the degenerative process of the salivary glands of *D. melanogaster* (Jiang et al., 2000).

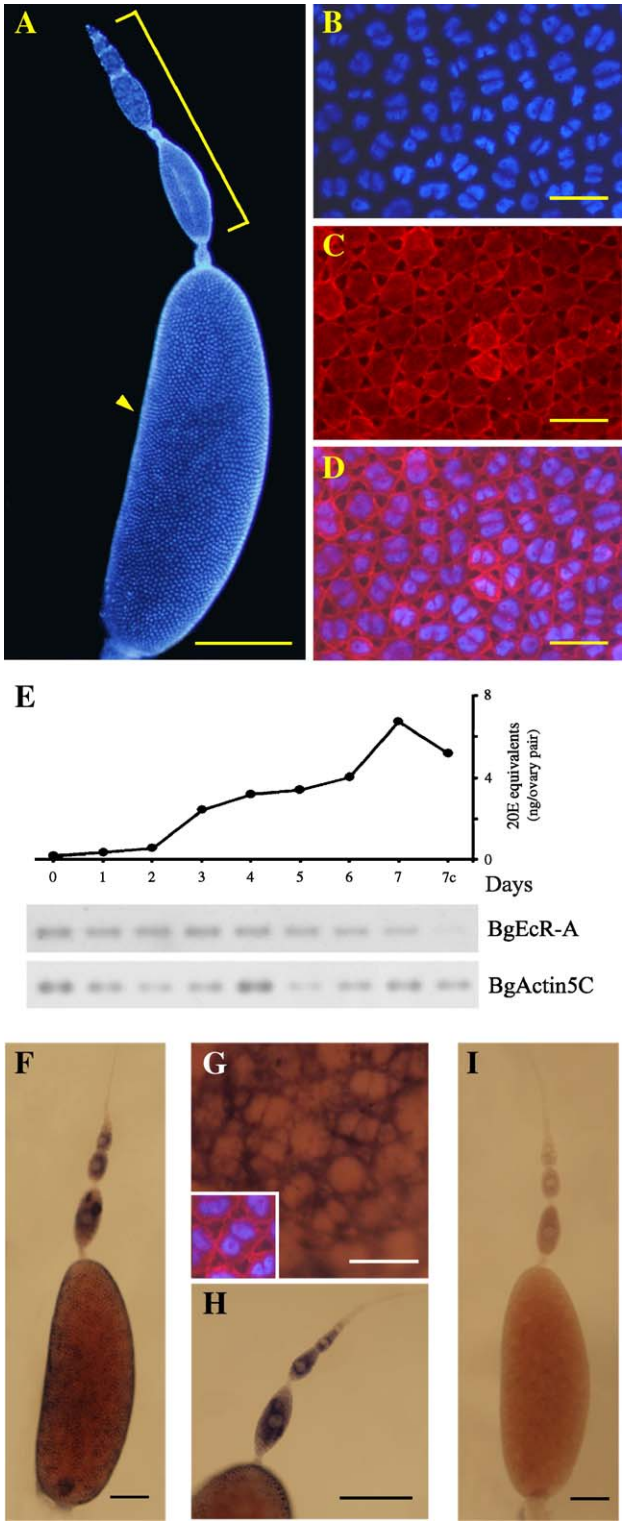

Fig. 9. Structure of the *B. germanica* panoistic ovary and expression of BgEcR-A. (A) Ovariole from a 5-day-old adult specimen. The basal oocyte (arrowhead) is the only one that develops during the adult stage, whereas the remaining oocytes keep immature (bracket). DAPI (in blue) was used to reveal the nuclei. Anterior–posterior axis is oriented up to down, and dorsal–ventral axis is oriented left to right. (B) DAPI staining of the follicular cells that surround the basal oocyte showing huge binucleate nuclei. (C) Phalloidin-tritc treatment of the same cells, showing strong staining in the cell periphery. Large intercellular spaces are well apparent. (D) Overlay of panels B and C. (E) Ovarian ecdysteroids and temporal expression pattern of BgEcR-A mRNA during oogenesis. Data on ovarian ecdysteroids are from Pascual et al. (1992). For mRNA pattern, equal amounts of total RNA from staged ovaries were analyzed by RT-PCR/Southern blotting using BgEcR-A-specific probes. BgActin5C mRNA levels were used as a reference. The Southern blots are representative of three replicates. 7c corresponds to 7-day-old females with chorionated oocytes. (F) Hybridizations in situ with an antisense BgEcR-A RNA probe on a 5-day-old ovariole. mRNA of BgEcR-A is detected in the follicular cells surrounding the basal oocyte. (G) Detail of the follicular cells showing that the BgEcR-A transcript is localized in the cytoplasm. The insert shows a DAPI-Phalloidin-tritc staining of the same cells. (H) BgEcR-A mRNA is also detected in the follicular epithelium of the sub-basal oocyte and in the more immature oocytes but not in the germanium and the terminal filament. (I) Control ovariole hybridized with sense BgEcR-A probe showing no staining. Scale bars: 250 μm in panels A, H; 50 μm in panels B–D, G; 125 μm in panels F, I.

BgEcR-A is involved in choriogenesis

In addition to the above phenotypes, adults that develop from BgEcR-A knockdown nymphs are sterile, but sterility is not due to an impairment of the vitellogenic process itself. Neither the synthesis of yolk protein precursors by the fat body, nor their release to the hemolymph or the incorporation into the developing oocytes is affected because the reduction of BgEcR-A levels during the adult stage did not alter the hemolymph or the ovarian levels of vitellogenin/vitellin. This is not surprising given that vitellogenesis of *B. germanica* is strictly dependent on juvenile hormone, whereas ecdysteroids do not play any apparent role on that process (Comas et al., 2001). A close examination revealed that oocytes from females treated with dsBgEcR-A degenerated at the onset of choriogenesis. Normally, synthesis of chorion proteins coincides with a dramatic structural reorganization of the follicular epithelium (Figs. 10D–G; see also Zhang and Kunkel, 1992; Romañá et al., 1995). This rearrangement is impaired in dsBgEcR-A-treated females (Fig. 11). Previous studies in vitro had demonstrated that 20E induces precocious choriogenesis in *B. germanica*

(Bellés et al., 1993), which is in agreement with the present results. Although no molecular evidence linking EcR and choriogenesis has been reported, Shea et al. (1990) have shown that USP, the heterodimeric partner of EcR, is involved in the synthesis of chorion proteins of *D. melanogaster*. Recently, Cherbas et al. (2003) have described that *D. melanogaster* ovaries defective in the 20E signaling in the polar and/or

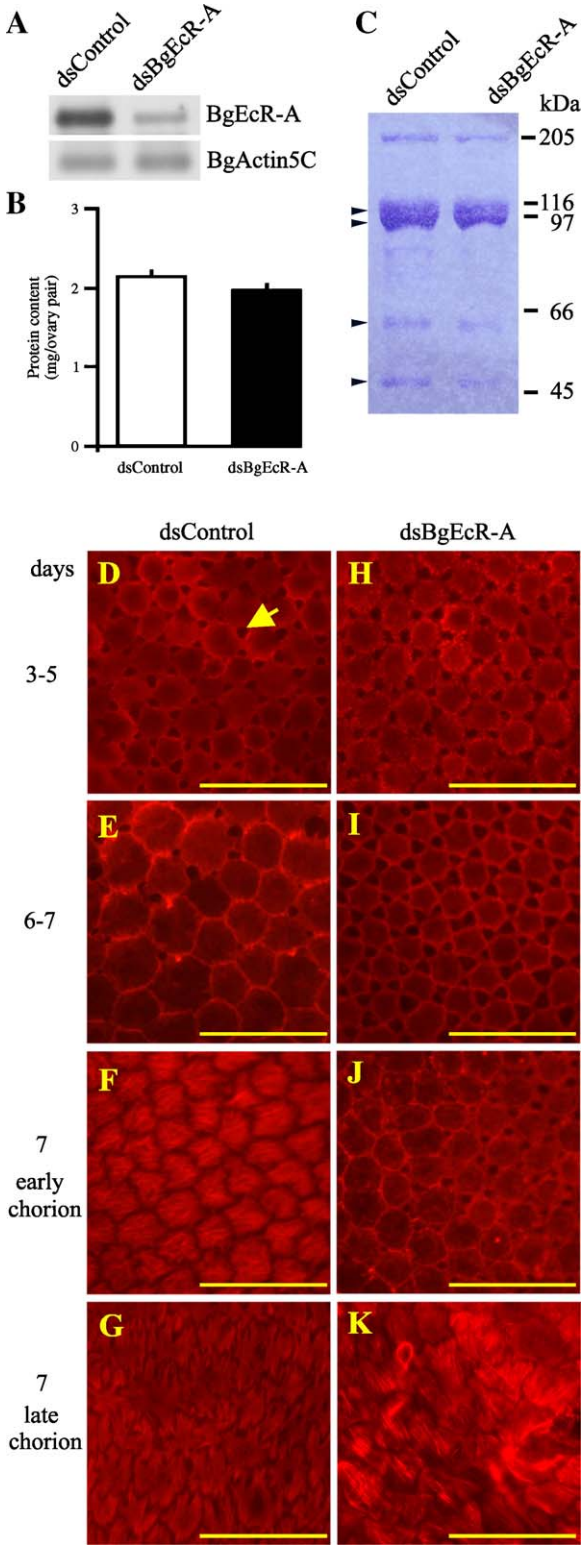

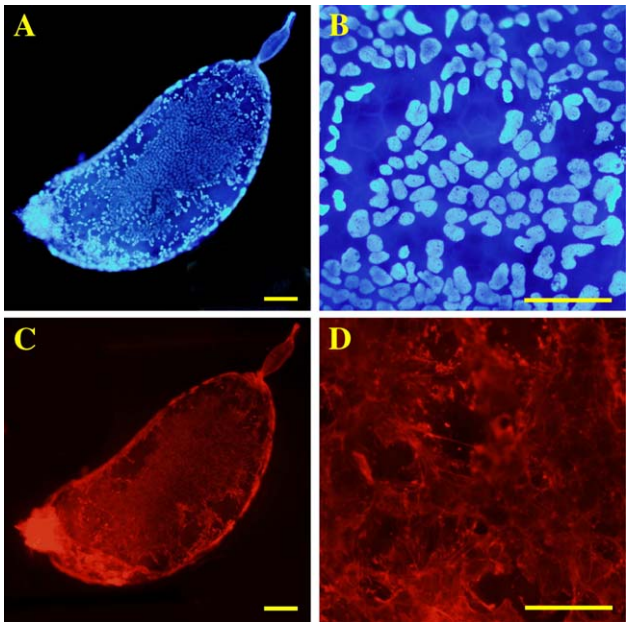

Fig. 11. RNAi-mediated knockdown of BgEcR-A in *B. germanica* adult females provokes the degeneration of the follicle at the onset of the choriogenesis. (A) DAPI staining and (C) phalloidin-tritc staining of a 7-day-old ovary from a adult female that had been treated with 1 μg of dsBgEcR-A after the imaginal molt, showing a clear degeneration of the follicular cells surrounding the basal oocyte. The sub-basal oocyte remained unaffected. Anterior–posterior axis is oriented up to down, and dorsal–ventral axis is oriented left to right. (B) DAPI staining of the nuclei from the follicular cells of the ovary shown in panel A. Nuclei are irregularly distributed, exhibit abnormal shapes and, in some cases, they are fused, thus indicating that cells are degenerating. (D) Phalloidin-tritc staining of the same section shown in panel B. Scale bars: 250 μm in panels A, C; 125 μm in panels B, D.

centripetal follicular cells show chorion defects, including chorion fragility and malformations of the operculum and dorsal appendages. Moreover, 20E signaling is required for oocyte progression to pass the mid-oogenesis checkpoint, and it is also needed within the germline for survival until late oogenesis of *D. melanogaster* (Buszczak et al., 1999). Finally, *EcR* mutant females of *D. melanogaster* show abnormal egg chambers and loss of vitellogenic egg stages (Carney and Bender, 2000). The 20E-induced hierarchy of transcription factors has also been

Fig. 10. Effect of RNAi-mediated knockdown of BgEcR-A in the oogenesis and choriogenesis of adult *B. germanica*. (A) BgEcR-A mRNA in dsBgEcR-A-treated specimens compared with dsControl-treated specimens in ovaries of adult *B. germanica*. 1 μg of dsBgEcR-A or dsControl was injected into abdomens of newly ecdysed adult females, and BgEcR-A mRNA levels were measured in the ovaries 6 days later by RT-PCR/Southern blot. (B) Protein content in the ovaries of dsControl and dsBgEcR-A-treated adult females 6 days after the treatment. (C) Electrophoretic analysis of ovaries from dsControl and dsBgEcR-A-treated adult females 6 days after the treatment. The gel is representative of 10 replicates—Differences observed in protein and vitellin are not significant. The arrowheads on the left indicate the subunits of vitellin (102, 95, 60 and 50 kDa). Molecular mass standards are shown on the right. (D–K) Reduction of BgEcR-A levels in the ovaries disrupt actin filament reorganization in the follicular cells at the onset of choriogenesis. Phalloidin-tritc staining of the follicular cells in dsBgEcR-A and dsControl-treated adult females between day 3 after the treatment and oviposition. Development in controls is represented in left panels (D–G) whereas that in dsBgEcR-A-treated specimens is shown in right panels (H–K). The arrow in panel D indicates the space intercellular spaces in the follicle. Scale bars: 100 μm.

detected during the oogenesis of the yellow fever mosquito, *A. aegypti* (Pierceall et al., 1999; Wang et al., 2000), and the silkmoth, *B. mori* (see Swevers and Iatrou, 2003).

In conclusion, we have developed a simple and reliable RNAi method in vivo to efficiently disrupt gene function in nymphs and adults of the hemimetabolous insect *B. germanica*. Disruption of *BgEcR-A* expression by this technique did not completely eliminate BgEcR-A mRNA, but most of the treated specimens exhibited phenotypic defects indicating that the BgEcR-A reduction achieved was enough to result in functional consequences. Given that one of these consequences was that ecdysteroid levels were reduced, one concern that can be considered is whether the phenotypes observed resulted from BgEcR-A reduction or from reduced 20E titer, or both. In any event, BgEcR-A is the receptor of 20E, which leads to conclude that it is the reduction in 20E signaling in the specimen that determines the observed phenotypes, an assumption that should also apply to the case of *D. melanogaster*. Indeed, hemolymph ecdysteroid titers have never been reported in the analysis of the EcR mutants described so far in the fruitfly. Moreover, in all cases described in *D. melanogaster*, the mutation of *EcR* produced a clear de-regulation of the expression of most 20E-responsive genes, thus making impossible to discern whether the reported phenotypes are directly due to the absence of EcR or to the absence of other 20E-dependent factors. Recently, Cherbas et al. (2003) have reported non-autonomous developmental blockages after the inactivation of *EcR* function in *D. melanogaster* via the overexpression of dominant negative forms of EcR. Most interestingly, the imaginal discs of these specimens were induced to develop by 20E treatment in vitro, which indicates that development failed because the ecdysteroid levels were insufficient.

We have focused our study on BgEcR-A, but we cannot rule out the occurrence of other EcR isoforms in *B. germanica*. Work directed to identify other possible isoforms is currently in progress in our laboratory. Nevertheless, the expression patterns obtained using a primer pair designed on the LBD domain, that would amplify all possible EcR isoforms, were parallel to those of BgEcR-A. In addition, the phenotypes observed either using a dsRNA designed on the A/B domain to target BgEcR-A, or a dsRNA designed on the LBD domain that would target any BgEcR isoform, were coincident. These data suggest that if there are other BgEcR isoforms, then they might have functions largely redundant with those of BgEcR-A. In any case, our study clearly indicates that BgEcR-A is crucial for developmental progression in the hemimetabolous insect *B. germanica*.

Acknowledgments

Financial support from the Spanish Ministry of Science and Technology (SMST), (projects BMC2002-03222 to D.M. and AGL2002-01169 to X.B.) and the Generalitat de Catalunya (GC) (2001 SGR 003245) is gratefully acknowledged. Thanks are due to Núria Pascual, from our department, for ecdysteroid measurements and to Patrick Porcheron (Université de Paris 6) for providing the AS 4919 antiserum. J.C. is recipient of a pre-doctoral research grant from CSIC (I3P) and D.M-P is recipient of a pre-doctoral research grant from the Spanish Ministry of Education and Science (MEC).

References

Bellés, X., Cassier, P., Cerdà, X., Pascual, N., André, M., Rosso, Y., Piulachs, M.D., 1993. Induction of choriogenesis by 20-hydroxyecdysone in the German cockroach. Tissue Cell 25, 195–204.

Bender, M., Imam, F.B., Talbot, W.S., Ganetzky, B., Hogness, D.S., 1997. *Drosophila* ecdysone receptor mutations reveal functional differences among receptor isoforms. Cell 91, 777–788.

Bialecki, M., Shilton, A., Fichtenberg, C., Segraves, W.A., Thummel, C.S., 2002. Loss of the ecdysteroid-inducible E75A orphan nuclear receptor uncouples molting from metamorphosis in *Drosophila*. Dev. Cell 3, 209–220.

Blandin, S., Moita, L.F., Kocher, T., Wilm, M., Kafatos, F.C., Levashina, E.A., 2002. Reverse genetics in the mosquito *Anopheles gambiae*: targeted disruption of the *Defensin* gene. EMBO Rep. 3, 852–856.

Bradford, M.M., 1976. A rapid and sensitive method for the quantitation of microgram quantities of protein utilizing the principle of Protein-Dye Binding. Anal. Biochem. 72, 248–254.

Bucher, G., Scholten, J., Klingler, M., 2002. Parental RNAi in *Tribolium* (Coleoptera). Curr. Biol. 12, R85–R86.

Buszczak, M., Freeman, M.R., Carlson, J.R., Bender, M., Cooley, L., Segraves, W.A., 1999. Ecdysone response genes govern egg chamber development during mid-oogenesis in *Drosophila*. Development 126, 4581–4589.

Carney, G.E., Bender, M., 2000. The *Drosophila* ecdysone receptor (EcR) gene is required maternally for normal oogenesis. Genetics 154, 1203–1211.

Champlin, D.T., Truman, J.W., 1998. Ecdysteroid control of cell proliferation during optic lobe neurogenesis in the moth *Manduca sexta*. Development 25, 269–277.

Cherbas, L., Hu, X., Zhimulev, I., Belyaeva, E., Cherbas, P., 2003. EcR isoforms in *Drosophila*: testing tissue-specific requirements by targeted blockade and rescue. Development 130, 271–284.

Comas, D., Piulachs, M.D., Bellés, X., 2001. Induction of vitellogenin gene transcription in vitro by juvenile hormone in *Blattella germanica*. Mol. Cell. Endocrinol. 183, 93–100.

Cruz, J., Martin, D., Pascual, N., Maestro, J.L., Piulachs, M.D., Bellés, X., 2003. Quantity does matter. Juvenile hormone and the onset of vitellogenesis in the German cockroach. Insect Biochem. Mol. Biol. 33, 1219–1225.

Dai, J.D., Gilbert, L.I., 1991. Metamorphosis of the corpus allatum and degeneration of the prothoracic glands during the larval-pupal-adult transformation of *Drosophila melanogaster*: a cytophysiological analysis of the ring gland. Dev. Biol. 144, 309–326.

Dai, J.D., Gilbert, L.I., 1997. Programmed cell death of the prothoracic glands of *Manduca sexta* during pupal–adult metamorphosis. Insect Biochem. Mol. Biol. 27, 69–78.

Davis, M.B., Carney, G.E., Robertson, A.E., Bender, M., 2005. Phenotypic analysis of EcR-A mutants suggests that EcR isoforms have unique functions during *Drosophila development*. Dev. Biol. 282, 385–396.

Dewey, E.M., McNabb, S.L., Ewer, J., Kuo, G.R., Takanishi, C.L., Truman, J.W., Honegger, H.W., 2004. Identification of the gene encoding bursicon, an insect neuropeptide responsible for cuticle sclerotization and wing spreading. Curr. Biol. 14, 1208–1213.

Gaziova, I., Bonnette, P.C., Henrich, V.C., Jindra, M., 2004. Cell-autonomous roles of the ecdysoneless gene in *Drosophila* development and oogenesis. Development 131, 2715–2725.

Gilbert, L.I., 2004. Halloween genes encode P450 enzymes that mediate steroid hormone biosynthesis in *Drosophila melanogaster*. Mol. Cell. Endocrinol. 215, 1–10.

Jiang, C., Lamblin, A.F., Steller, H., Thummel, C.S., 2000. A steroid-triggered transcriptional hierarchy controls salivary gland cell death during *Drosophila* metamorphosis. Mol. Cell 5, 445–455.

Jindra, M., Riddiford, L.M., 1996. Expression of ecdysteroid-regulated transcripts in the silk gland of the wax moth, *Galleria mellonella*. Dev. Genes Evol. 206, 305–314.

Jindra, M., Malone, F., Hiruma, K., Riddiford, L.M., 1996. Developmental profiles and ecdysteroid regulation of the mRNAs for two ecdysone receptor isoforms in the epidermis and wings of the tobacco hornworm, *Manduca sexta*. Dev. Biol. 180, 258–272.

Karim, F.D., Thummel, C.S., 1992. Temporal coordination of regulatory gene expression by the steroid hormone ecdysone. EMBO J. 11, 4083–4093.

Kennerdell, J.R., Carthrew, R.W., 2000. Heritable gene silencing in *Drosophila* using double-stranded RNA. Nat. Biotech. 17, 896–898.

King-Jones, K., Thummel, C.S., 2005. Nuclear receptors-a perspective from *Drosophila*. Nat. Rev., Genet. 6, 311–323.

Koelle, M.R., Talbot, W.S., Segraves, W.A., Bender, M.T., Cherbas, P., Hogness, D.S., 1991. The *Drosophila* EcR gene encodes an ecdysone receptor, a new member of the steroid receptor superfamily. Cell 67, 59–77.

Kothapalli, R., Palli, S.R., Ladd, T.R., Sohi, S.S., Cress, D., Dhadialla, T.S., Tzertzinis, G., Retnakaran, A., 1995. Cloning and developmental expression of the ecdysone receptor gene from the spruce budworm, *Choristoneura fumiferana*. Dev. Genet. 17, 319–330.

Lam, G., Thummel, C.S., 2000. Inducible expression of double-stranded RNA directs specific genetic interference in *Drosophila*. Curr. Biol. 10, 957–963.

Maestro, O., Cruz, J., Pascual, N., Martín, D., Bellés, X., 2005. Differential expression of two RXR/ultraspiracle isoforms during the life cycle of the hemimetabolous insect *Blattella germanica* (Dictyoptera, Blattellidae). Mol. Cell. Endocrinol. 238, 27–37.

Marie, B., Bacon, J.P., Blagburn, J.M., 2000. Double-stranded RNA interference shows that Engrailed controls the synaptic specificity of identified sensory neurons. Curr. Biol. 10, 289–292.

Martín, D., Piulachs, M.D., Bellés, X., 1995. Patterns of haemolymph vitellogenin and ovarian vitellin in the German cockroach, and the role of juvenile hormone. Physiol. Entomol. 20, 59–65.

McNabb, S.L., Baker, J.D., Agapite, J., Steller, H., Riddiford, L.M., Truman, J.W., 1997. Disruption of a behavioral sequence by targeted death of peptidergic neurons in *Drosophila*. Neuron 19, 813–823.

Montgomery, M.K., Xu, S., Fire, A., 1998. RNA as a target of double-stranded RNA-mediated genetic interference in *Caenorhabditis elegans*. Proc. Natl. Acad. Sci. U. S. A. 95, 15502–15507.

Mottier, V., Siaussat, D., Bozzolan, F., Auzoux-Bordenave, S., Porcheron, P., Debernard, S., 2004. The 20-hydroxyecdysone-induced cellular arrest in G2 phase is preceded by an inhibition of cyclin expression. Insect Biochem. Mol. Biol. 34, 51–60.

Neubueser, D., Warren, J.T., Gilbert, L.I., Cohen, S.M., 2005. *molting defective* is required for ecdysone biosynthesis. Dev. Biol. 280, 362–372.

Park, J.H., Schroeder, A.J., Helfrich-Forster, C., Jackson, F.R., Ewer, J., 2003. Targeted ablation of CCAP neuropeptide-containing neurons of *Drosophila* causes specific defects in execution and circadian timing of ecdysis behavior. Development 130, 2645–2656.

Pascual, N., Cerdà, X., Benito, B., Tomás, J., Piulachs, M.D., Bellés, X., 1992. Ovarian ecdysteroids levels and basal oocyte development during maturation in the cockroach *Blattella germanica* (L.). J. Insect Physiol. 38, 339–348.

Perera, S.C., Ladd, T.R., Dhadialla, T.S., Krell, P.J., Sohi, S.S., Retnakaran, A., Palli, S.R., 1999. Studies on two ecdysone receptor isoforms of the spruce budworm, *Choristoneura fumiferana*. Mol. Cell. Endocrinol. 152, 73–84.

Pierceall, W.E., Li, C., Biran, A., Miura, K., Raikhel, A.S., Segraves, W.A., 1999. E75 expression in mosquito ovary and fat body suggests reiterative use of ecdysone-regulated hierarchies in development and reproduction. Mol. Cell. Endocrinol. 25, 73–89.

Porcheron, P., Morinière, N., Grassi, J., Pradelles, P., 1989. Development of an enzyme immunoassay for ecdysteroids using acetyl-cholinesterase as label. Insect Biochem. 19, 117–122.

Riddiford, L., Cherbas, P., Truman, J.W., 2001. Ecdysone receptors and their biological actions. Vitam. Horm. 60, 1–73.

Romañá, I., Pascual, N., Bellés, X., 1995. The ovary is a source of circulating ecdysteroids in *Blattella germanica* (L.) (Dictyoptera, Blattellidae). Eur. J. Entomol. 92, 93–103.

Rusten, T.E., Lindmo, K., Juhasz, G., Sass, M., Seglen, P.O., Brech, A., Stenmark, H., 2004. Programmed autophagy in the *Drosophila* fat body is induced by ecdysone through regulation of the PI3K pathway. Dev. Cell 7, 179–192.

Schubiger, M., Wade, A.A., Carney, G.E., Truman, J.W., Bender, M., 1998. *Drosophila* EcR-B ecdysone receptor isoforms are required for larval molting and for neuron remodeling during metamorphosis. Development 125, 2053–2062.

Scott, R.C., Schuldiner, O., Neufeld, T.P., 2004. Role and regulation of starvation-induced autophagy in the *Drosophila* fat body. Dev. Cell 7, 167–178.

Shea, M.J., King, D.L., Conboy, M.J., Mariani, B.D., Kafatos, F.C., 1990. Proteins that bind to *Drosophila* chorion *cis*-regulatory elements: a new C_2H_2 zinc finger protein and a C_2C_2 steroid receptor-like component. Genes Dev. 4, 1128–1140.

Shin, S.W., Kokoza, V.A., Raikhel, A.S., 2003. Transgenesis and reverse genetics of mosquito innate immunity. J. Exp. Biol. 206, 3835–3843.

Sullivan, A.A., Thummel, C.S., 2003. Temporal profiles of nuclear receptor gene expression reveal coordinate transcriptional responses during *Drosophila* development. Mol. Endocrinol. 17, 2125–2137.

Swevers, L., Iatrou, K., 2003. The ecdysone regulatory cascade and ovarian development in lepidopteran insects: insights from the silkmoth paradigm. Insect Biochem. Mol. Biol. 33, 1285–1297.

Talbot, W.S., Swyryd, E.A., Hogness, D.S., 1993. *Drosophila* tissues with different metamorphic responses to ecdysone express different ecdysone receptor isoforms. Cell 73, 1323–1337.

Thummel, C.S., 1995. From embryogenesis to metamorphosis: the regulation and function of *Drosophila* nuclear receptor superfamily members. Cell 83, 871–877.

Thummel, C.S., 2001. Steroid-triggered death by autophagy. BioEssays 23, 677–682.

Tomoyasu, Y., Denell, R.E., 2004. Larval RNAi in *Tribolium* (Coleoptera) for analyzing adult development. Dev. Genes Evol. 214, 575–578.

Verras, M., Gourzi, P., Zacharopoulou, A., Mintzas, A.C., 2002. Developmental profiles and ecdysone regulation of the mRNAs for two ecdysone receptor isoforms in the Mediterranean fruit fly *Ceratitis capitata*. Insect Mol. Biol. 11, 553–565.

Wang, S.F., Li, C., Zhu, J., Miura, K., Miksicek, R.J., Raikhel, A.S., 2000. Differential expression and regulation by 20-hydroxyecdysone of mosquito ultraspiracle isoforms. Dev. Biol. 1, 99–113.

Wang, S.F., Li, C., Sun, G., Zhu, J., Raikhel, A.S., 2002. Differential expression and regulation by 20-hydroxyecdysone of mosquito ecdysteroid receptor isoforms A and B. Mol. Cell. Endocrinol. 196, 29–42.

Yao, T.P., Forman, B.M., Jiang, Z., Cherbas, L., Chen, J.D., McKeown, M., Cherbas, P., Evans, R.M., 1993. Functional ecdysone receptor is the product of EcR and Ultraspiracle genes. Nature 366, 476–479.

Yin, V.P., Thummel, C.S., 2005. Mechanisms of steroid-triggered programmed cell death in *Drosophila*. Semin. Cell Dev. Biol. 16, 237–243.

Zhang, Y., Kunkel, J.G., 1992. Program of F-actin in the follicular epithelium during oogenesis of the German cockroach, *Blattella germanica*. Tissue Cell 24, 905–917.

Zhou, X., Zhou, B., Truman, J.W., Riddiford, L.M., 2004. Overexpression of broad: a new insight into its role in the *Drosophila* prothoracic gland cells. J. Exp. Biol. 207, 1151–1161.

Zitnan, D., Adams, M.E., 2005. Neuroendocrine regulation of insect ecdysis. In: Gilbert, L.I., Iatrou, K., Gill, S.S. (Eds.), Comprehensive Molecular Insect Science, vol. 3. Elsevier Pergamon, pp. 1–60.